RESEARCH PAPER

Nucleus 5:6, 527–541; November/December 2014; © 2014 Taylor & Francis Group, LLC

Cellular stress induces Bax-regulated nuclear bubble budding and rupture followed by nuclear protein release

Liora Lindenboim[1], Tiki Sasson[1], Howard J Worman[2], Christoph Borner[3,4,5], and Reuven Stein[1,*]

[1]Department of Neurobiology; George S. Wise Faculty of Life Sciences; Tel Aviv University; Ramat Aviv, Israel; [2]Department of Medicine and Department of Pathology and Cell Biology; College of Physicians and Surgeons; Columbia University; New York, NY, USA; [3]Institute of Molecular Medicine and Cell Research; Albert Ludwigs University Freiburg; Freiburg, Germany; [4]Spemann Graduate School of Biology and Medicine (SGBM); Albert Ludwigs University Freiburg; Freiburg, Germany; [5]Excellence Cluster, Centre for Biological Signaling Studies (BIOSS); Albert Ludwigs University Freiburg; Freiburg, Germany

Keywords: apoptosis, Bax, lamin, nuclear envelope, nucleus

Abbreviations: KASH, Klarsicht: ANC-1, Syne homology; NE, nuclear envelope; INM, inner nuclear membrane; ONM, outer nuclear membrane; NPCs, nuclear pore complexes; LAP, lamina-associated polypeptide; LINC, links nucleoskeleton and cytoskeleton; Bax/Bak, Bax and Bak; MOMP, mitochondrial outer membrane permeabilization; NPR, nuclear protein redistribution; MEFs, mouse embryonic fibroblasts; PI, propidium iodide; SIGRUNB, stress-induced generation and rupture of nuclear bubbles; NPM, nucleophosmin; DKO, double knockout; Q-VD-OPH, quinoline-Val-Asp(OMe)-CH_2-OPH.

Cellular stress triggers many pathways including nuclear protein redistribution. We previously discovered that this process is regulated by Bax but the underlying mechanism has not yet been studied. Here we define this mechanism by showing that apoptotic stimuli cause Bax-regulated disturbances in lamin A/C and nuclear envelope (NE)-associated proteins which results in the generation and subsequent rupture of nuclear protein-containing bubbles. The bubbles do not contain DNA and are encapsulated by impaired nuclear pore-depleted NE. Stress-induced generation and rupture of nuclear bubbles ultimately leads to the discharge of nuclear proteins into the cytoplasm. This process precedes morphological changes of apoptosis and occurs independently of caspases. Rescue experiments revealed that this Bax effect is non-canonical, i.e. it requires the BH3 domain and α-helices 5 and 6 but it is not inhibited by Bcl$^-$x$_L$. Targeting Bax to the NE by the Klarsicht/ANC-1/Syne-1 homology (KASH) domain effectively triggers the generation and rupture of nuclear bubbles. Overall, our findings provide evidence for a novel stress-response, which is regulated by a non-canonical action of Bax on the NE.

Introduction

In eukaryotes, the nuclear envelope (NE) separates the nuclear content from the cytosol. The NE is comprised of inner and outer nuclear membranes (INM and ONM, respectively), which are separated by the perinuclear space. It is generally accepted that nucleocytoplasmic traffic across the NE occurs via nuclear pore complexes (NPCs).[1,2] Below the INM is the nuclear lamina, a meshwork of intermediate filament proteins termed lamins (both A and B types) which provide structural support to the nucleus and regulates transcription and chromatin organization.[3-5] The lamins bind to numerous proteins, such as lamina-associated polypeptide (LAP) 2β, emerin, SUN1 and SUN2. Some are INM proteins that help anchor lamin filaments to the NE. Others bind partners in the ONM and mechanically connect lamins to the cytoskeleton.[6] The SUN proteins span the INM to the NE lumen where they interact with ONM-embedded cytoskeleton-interacting proteins termed Klarsicht, ANC-1, Syne homology (KASH)-domain proteins (nesprins in mammals) to form linker of nucleoskeleton and cytoskeleton (LINC) complexes.

Apoptosis proceeds via either intrinsic or extrinsic apoptotic pathways, both leading to the activation of caspases, which cleave diverse sets of proteins.[7] The intrinsic pathway is regulated by the Bcl$^-$2 protein family, of which the pro-apoptotic members Bax and Bak (Bax/Bak) cause mitochondrial outer membrane permeabilization (MOMP). This leads to the release of mitochondrial proteins such as cytochrome *c*, which in turn form a cytosolic, caspase-9-containing protein complex (apoptosome) that cleaves and activates the effector caspase-3. Whereas Bax/Bak are in an inactive conformation in healthy cells, they undergo structural changes in response to apoptotic stimuli, which lead to their activation and subsequent MOMP. The triggers/mediators for Bax/Bak activation are the BH3-only proteins, whereas anti-apoptotic proteins such as Bcl$^-$2, Bcl$^-$x$_L$ and Mcl$^-$1 inhibit this activation.[8]

*Correspondence to: Reuven Stein; Email: reuvens@post.tau.ac.il
Submitted: 06/18/2014; Revised: 07/31/2014; Accepted: 09/15/2014
http://dx.doi.org/10.4161/19491034.2014.970105

The NE is perforated in response to apoptotic stresses, leading to the redistribution of nuclear proteins to the cytosol.[9,10] This perforation has been suggested to be caused by NPCs dismantling mediated by caspase-dependent proteolysis of a subset of nucleoporins[11-15] or by calpains during excitotoxic neuronal death.[16] However, we have recently shown that stress-induced nuclear protein redistribution (NPR) in mouse embryonic fibroblasts (MEFs) is regulated by Bax/Bak in a non-canonical manner, i.e., independent of caspases and non-inhibitable by $Bcl\text{-}x_L$.[17] We therefore reasoned that this process is mediated by a NPCs-independent mechanism. In this study, we provide the molecular mechanism of this NPC-independent NPR. We show that apoptotic/stress stimuli induce disturbances in the NE which lead to the budding of nuclear-associated bubbles. These bubbles are surrounded by NPC-lacking NE and filled with nuclear proteins but not with DNA. After their generation, these bubbles rupture and discharge their protein content into the cytosol. This process is regulated by Bax/Bak but not by $Bcl\text{-}x_L$ or caspases, and occurs before the appearance of late-onset apoptotic events. Both the BH3 and α-helices 5/6 domains of Bax are required for the effect of Bax on SIGRUNB. Moreover, targeting Bax to the NE via the KASH domain is sufficient to induce this process although an action of Bax from other subcellular sites cannot be excluded.

Results

Apoptotic stimuli induce generation and rupture of nuclear bubbles

We previously showed that apoptotic stimuli, such as genotoxic agents, promote redistribution of nucleolin and other nuclear proteins in a Bax/Bak-dependent manner.[17,18] To unravel the mechanism underlying this process, we used live cell imaging to follow the efflux of a fluorescent nuclear protein, GFP-nucleolin from the nucleus to the cytosol in MEFs stably expressing GFP-nucleolin (GN-WT MEFs) (**Fig. 1A**). Upon treating with cisplatin, some of these cells exhibited GFP-nucleolin-containing bubbles, which protruded from the surface of the nuclear membrane. Shortly after their appearance, these bubbles ruptured and their content was released into the cytosol (**Fig. 1B** and Vid. S1). At start (t = 00:00), GFP-nucleolin was exclusively confined to the nucleus. Thereafter, a GFP-nucleolin-containing bubble suddenly appeared at the apex of the nucleus and after 2.5 min, this bubble ruptured, releasing its GFP-nucleolin content into the cytoplasm. Quantitative analysis revealed that 28% of cisplatin-treated GN-WT MEFs underwent stress-induced generation and rupture of nuclear bubbles (herein SIGRUNB) during the recording time (**Table S1**). On average the bubble life time from its appearance to its rupture was 4.4 ± 1.2 min (mean ± SE; n = 18) and the size of the bubble at the time of rupture was 11.43 ± 1.42 μm^2 (mean ± SE; n = 18). Immunofluorescence microscopic analysis of fixed cells showed that the stress-induced nuclear bubbles contained endogenous nuclear proteins as indicated by the presence of nucleophosmin (NPM), histone H1 and PGC-1α (transcription coactivator) (Supplementary Material **Fig. S1**). However, the bubble lacked DNA because it was not stained with Hoechst. To examine if this was also the case in intact cells, the membrane permeable DNA binding dye Hoechst 33342 was added to the culture medium. The nuclear staining pattern with Hoechst 33342 did not change during bubble formation and rupture, and Hoechst 33342 did not stain the bubble (**Fig. 1C**). Next we examined whether SIGRUNB preceded or followed the appearance of typical late onset features of apoptosis such as plasma membrane blebbing, nuclear condensation and loss of plasma membrane integrity. As we show for a representative GFP-nucleolin expressing cell (**Fig. 2A** and Vid. S2), it had a healthy-appearing nucleus at t = 00:00; 30 s later, GFP-nucleolin spilled into the cytosol from the upper part of the cell, probably due to rupture of an undetectable bubble or by other mechanism; 114 min later, a bubble was generated and then ruptured within 2 min. During the recording time, cellular (as judged by cytosolic GFP-nucleolin staining) and nuclear morphologies looked normal. Importantly, the cell began to exhibit apoptotic features, such as nuclear shrinkage and plasma membrane blebbing only after 142 min.

To examine the relationship between SIGRUNB and the loss of plasma membrane integrity, cisplatin-treated GN-WT MEFs were incubated with the non-membrane permeable DNA binding dye propidium iodide (PI). Before (t = 00:00), during (t = 09:00 and 09:30) and also after (t = 120:00) SIGRUNB, the nucleus had a normal morphology and the cell was not stained with PI (**Fig. 2B** and Vid. S3). The absence of PI staining was not due to technical problems since the dye clearly stained the apoptotic nuclei of neighboring GFP-nucleolin-negative cells (**Fig. 2B** and Vid S3). Similar results were obtained when membrane integrity was assessed by additional non-membrane permeable DNA binding dye Hoechst 33258 (**Fig S2**). Assessment of the time period from the appearance of the bubble until appearance of nuclear condensation (a late apoptotic event), revealed that on the average nuclear condensation occurs 65.58 ± 12.7 [(mean ± SE) (n = 17)] min after bubble formation. We used an additional marker of late apoptosis, which is the loss of mitochondrial membrane potential and the appearance of unhealthy, fragmented mitochondria. After staining with MitoTracker® Red (a mitochondrial marker and indicator of membrane potential), a cell undergoing SIGRUNB showed a similar degree of intact mitochondria as a neighboring cell which did not exert SIGRUNB (**Fig. S3**). By contrast, a late apoptotic cell in the same field (marked by asterisk) did not seem to contain healthy mitochondria any more. Taken together, our results suggest that stress-induced nuclear bubbles contain nuclear proteins but no DNA and that they appear and rupture before typical signs of late apoptosis, i.e. mitochondrial membrane depolarization, nuclear condensation, plasma membrane blebbing and permeabilization.

To determine if bubble formation and rupture is a general response to cellular stress, we treated the GN-WT MEFs with another drug, camptothecin. We found that this agent also triggered the process (**Fig. S4**), with 29% of the cells exhibiting SIGRUNB during the recording time (**Table S1**). As before, no GFP-nucleolin bubbles appeared in the untreated cells during the same period indicating that SIGRUNB was a direct response to stress.

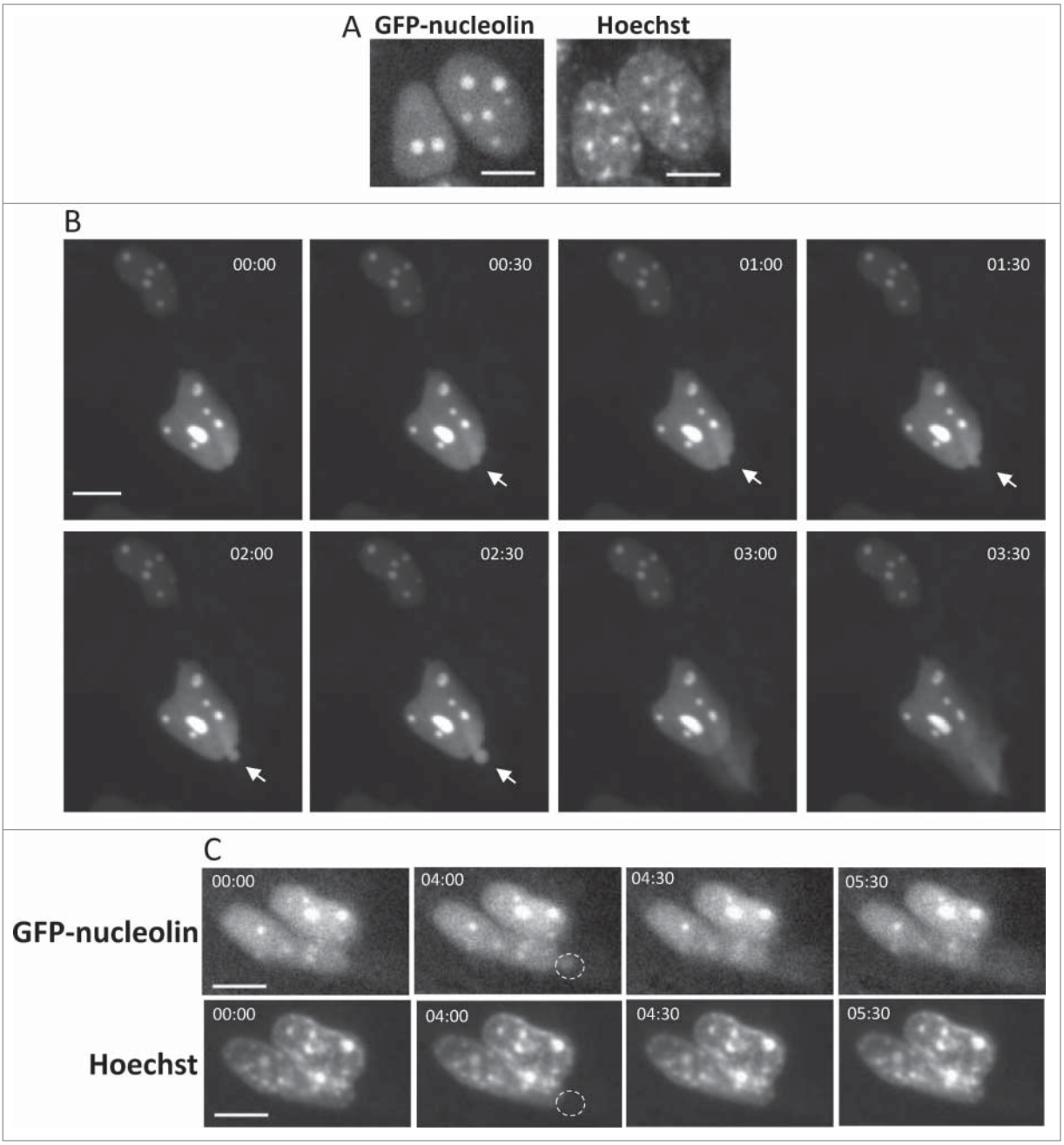

Figure 1. Cisplatin-treated GN-WT MEFs exhibiting SIGRUNB. (**A**) Expression of GFP-nucleolin in healthy GN-WT MEFs is confined to the nucleus. Hoechst 33342 was added to the culture medium of GN-WT MEFs and GFP-nucleolin and Hoechst fluorescence were monitored in live cells. GN-WT MEFs were treated with 25 μM cisplatin and after 15–24 h were subjected to live-cell imaging at 30-s intervals. (**B**) Appearance and subsequent rupture of GFP-nucleolin-containing nuclear bubble. The still images shown were taken from Vid. S1. Arrow indicates a bubble. The indicated time points (min:s) are expressed relative to the first image selected for presentation (t = 00:00), which corresponds to the image captured 34 min into the recording. (**C**) Stress-induced nuclear bubbles do not contain DNA. Hoechst 33342 was added to the culture medium 18 h after cisplatin treatment. Results shown (still images from time lapse imaging) are from the same field visualized separately for detection of GFP-nucleolin (upper panel) and Hoechst 33342 (lower panel). Dashed oval indicates the position of the nuclear bubble that lacks Hoechst 33342 staining. Indicated time points (min:s) are expressed as described in A. t = 00:00 corresponds to the image captured 43 min into the recording. The images shown are from representative experiments from 3, 8 and 8 independent experiments for A, B and C respectively.

SIGRUNB is Regulated by Bax/Bak

To examine whether SIGRUNB is associated with the previously discovered stress-induced NPR effect,[17,18] we tested its dependence on Bax/Bak. Bax/Bak double-knockout (DKO) MEFs stably expressing nuclear GFP-nucleolin (GN-DKO MEFs) were established and the effect of cisplatin or camptothecin on SIGRUNB was analyzed by live-cell imaging. As seen

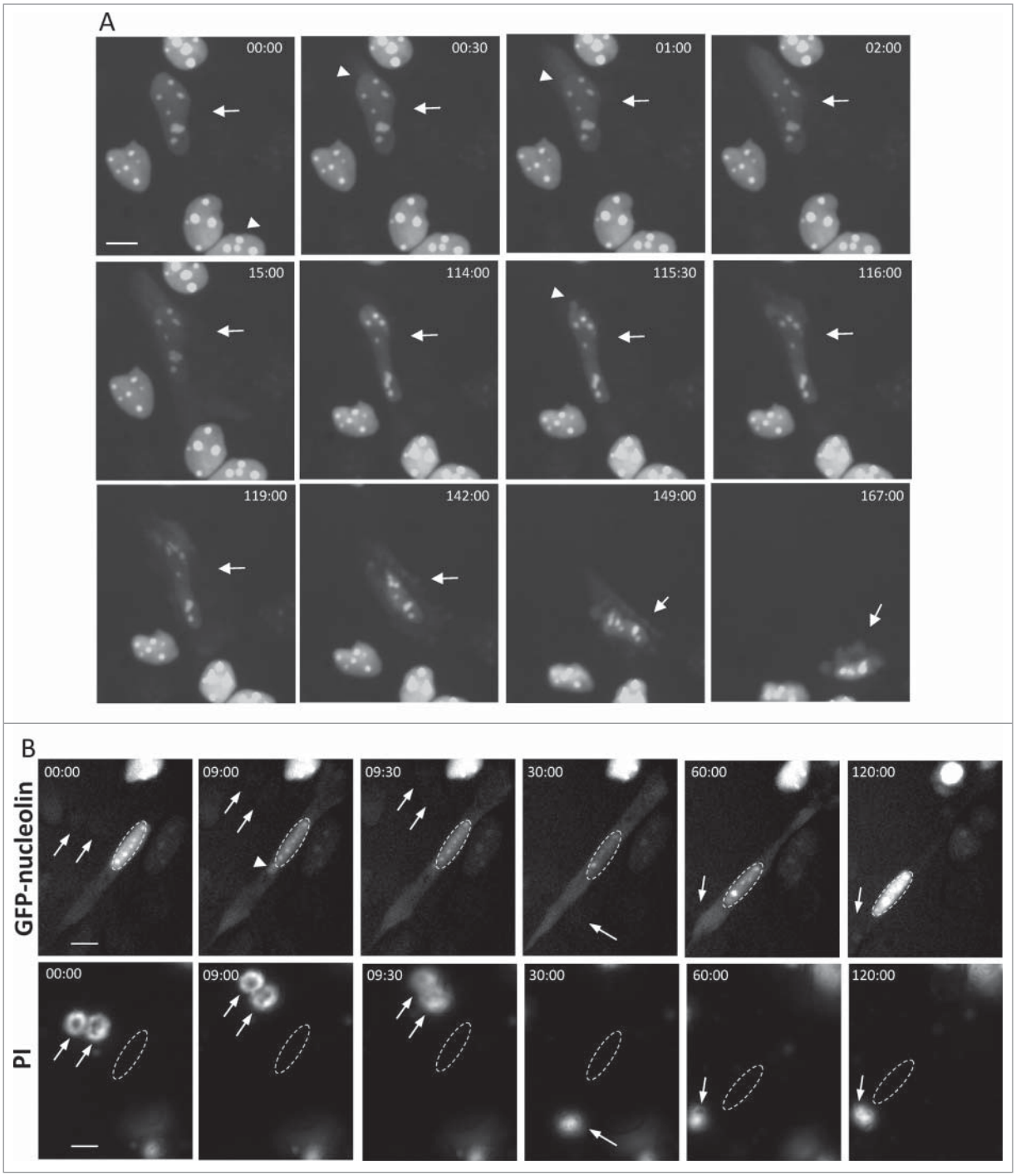

Figure 2. SIGRUNB preceded the appearance of typical late onset features of apoptosis (**A**) SIGRUNB occurs before the appearance of membrane blebbing and bubbling and nuclear condensation. The still images shown were taken from Vid. S2. Arrow indicates a cell undergoing SIGRUNB. Arrowhead points to a GFP-nucleolin-containing nuclear bubble. Indicated time points (min:s) are expressed as described in **Figure 1**. t = 00:00 corresponds to the image captured 50 min into the recording. (**B**) SIGRUNB occurs before loss of plasma-membrane integrity. PI was added to the culture medium 17 h after cisplatin treatment. The still images shown were taken from Vid. S3 and are from the same field visualized separately for detection of GFP-nucleolin (upper panel) and PI (lower panel). The images show a GFP-nucleolin-expressing cell which developed nuclear bubble (arrowhead) that burst shortly thereafter. No PI staining was observed in this cell at any of the time points shown. The position of the cell nucleus undergoing SIGRUNB is shown by dashed oval and is also superimposed on the PI images. Arrows indicate PI stained apoptotic nuclei of neighboring GFP-nucleolin-negative cells (the position of those cells is shown both in the PI panel and also when superimposed on the GFP-nucleolin images). Indicated time points (min:s) are expressed as describe in **Figure 1**. t = 00:00 corresponds to the image captured at the beginning of the recording. The images shown are from representative experiments from 8 and 3 independent experiments for A and B respectively. Bar = 10 μm.

before, GFP-nucleolin was mainly localized in the nucleus of untreated GN-DKO MEFs (**Fig. 3**). However, in contrast to GN-WT MEFs, neither cisplatin nor camptothecin provoked any nuclear bubble formation and rupture in GN-DKO MEFs during the recording time (**Table S1**; **Fig. 3**), indicating that Bax/Bak are needed for SIGRUNB induced by these stressors.

To further explore the mechanism underlying the effect of Bax/Bak on SIGRUNB we focused on Bax and investigated whether SIGRUNB can be rescued upon Bax re-expression in Bax/Bak DKO MEFs. Cells were co-transfected with RFP-nucleolin and GFP-Bax (or pEGFP as a control) and the cells' ability to undergo SIGRUNB was determined by live cell imaging. As previously reported,[17], the transient transfection procedure already provides a stress signal that can lead to SIGRUNB. Transfection of GFP-Bax induced the generation and subsequent rupture of bubbles containing RFP-nucleolin, but not DNA (**Fig. 4A** and Vid. S4). Again, this process preceded the appearance of apoptotic features. Transfection of the control vector pEGFP also induced some nuclear bubbles, but the percentage of cells exhibiting SIGRUNB during recording was substantially [24% (pEGFP) versus 60% (GFP-Bax)] and significantly ($p = 0.001$, Fisher's exact test) lower (**Fig. 4D**) than in GFP-Bax transfected cells. Notably, the average lifespan of GFP-Bax-induced bubbles in Bax/Bak DKO MEFs was longer than in cisplatin- or camptothecin-treated GN-WT cells (53.9 ± 8 min) and the size of the bubble at the time of rupture was extended as well [42.27 ± 7.66 μm^2 (mean ± SE; n = 14)]. Thus, re-expression of Bax in Bax/Bak DKO MEFs restored these cells' ability to undergo effective SIGRUNB although the process was somewhat slower. This reinforces the notion that Bax plays an important role in this process.

We next examined whether Bax-induced SIGRUNB is independent of caspases and Bcl^-x_L. Both Bax/Bak DKO MEFs transfected with GFP-Bax and treated with the general caspase inhibitor Q-VD-OPH (**Fig. 4B**) or co-transfected with GFP-Bax and Bcl^-x_L (**Fig. 4C**) exhibited characteristic SIGRUNB and showed no difference (Fisher's exact test) in the number of nuclear bubbles in these cells as compared to untreated MEFs expressing GFP-Bax only (**Fig. 4D**). By contrast, as previously reported,[19] Q-VD-OPH treatment and Bcl^-x_L overexpression inhibited cell death induced by GFP-Bax expression as indicated by the healthy appearance of the transfected cells. Therefore, Bax-induced SIGRUNB proceeds in a non-canonical manner, i.e., independent of caspases and unaffected by Bcl^-x_L overexpression.

Bax Mediates SIGRUNB Via Distinct Domains

To further characterize the mechanism by which Bax regulates SIGRUNB, we tested the effect of Bax domains needed for MOMP[20-23] and NPR.[18] Bax/Bak DKO MEFs were transfected with RFP-nucleolin together with GFP-tagged WT Bax or Bax mutants L63E (in the BH3 domain), ΔIGDE (deletion of critical amino acids in the BH3 domain), Δα5/6 (deletion of α helices 5/6) and 63-65A (region in BH3 essential for homo-oligomerization). At 24 h post-transfection, SIGRUNB was examined in fixed cells by assessing the following 3 parameters: (1) percentage of cells which retained RFP-nucleolin in the nucleus, (2) percentage of cells exhibiting nuclear bubbles containing RFP-nucleolin but no DNA, and (3) percentage of cells containing cytosolic RFP-nucleolin (which is indicative of bubble rupture). In accordance with the results obtained by live cell imaging, re-expression of GFP-Bax in Bax/Bak DKO MEFs significantly increased the percentage of cells exhibiting cytosolic RFP-nucleolin and decreased the percentage of cells exhibiting nuclear RFP-nucleolin as compared to

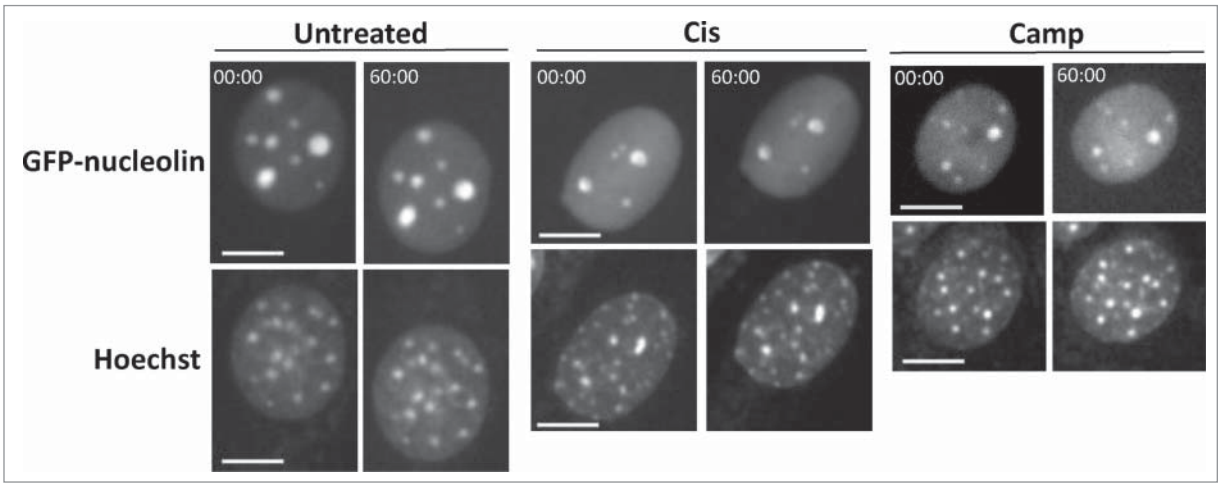

Figure 3. Bax/Bak are needed for SIGRUNB. GN-DKO MEFs were treated with 25 μM cisplatin (Cis) or 1 μM camptothecin (Camp) or left untreated. After 18 h, Hoechst 33342 was added to the culture medium and GFP-nucleolin and Hoechst fluorescence were monitored as described in **Figure 1**. The results shown (still images from time lapse imaging) are from the same field visualized separately for detection of GFP-nucleolin (upper panels) and Hoechst 33342 (lower panels). Indicated time points (min:s) are expressed relative to the first image selected for presentation (t = 00:00) which corresponds to the image captured at the beginning of the recording. Bar = 10 μm. The images shown are from representative experiments from 2, 3 and 2 independent experiments for untreated, Cis and Camp treated cells, respectively.

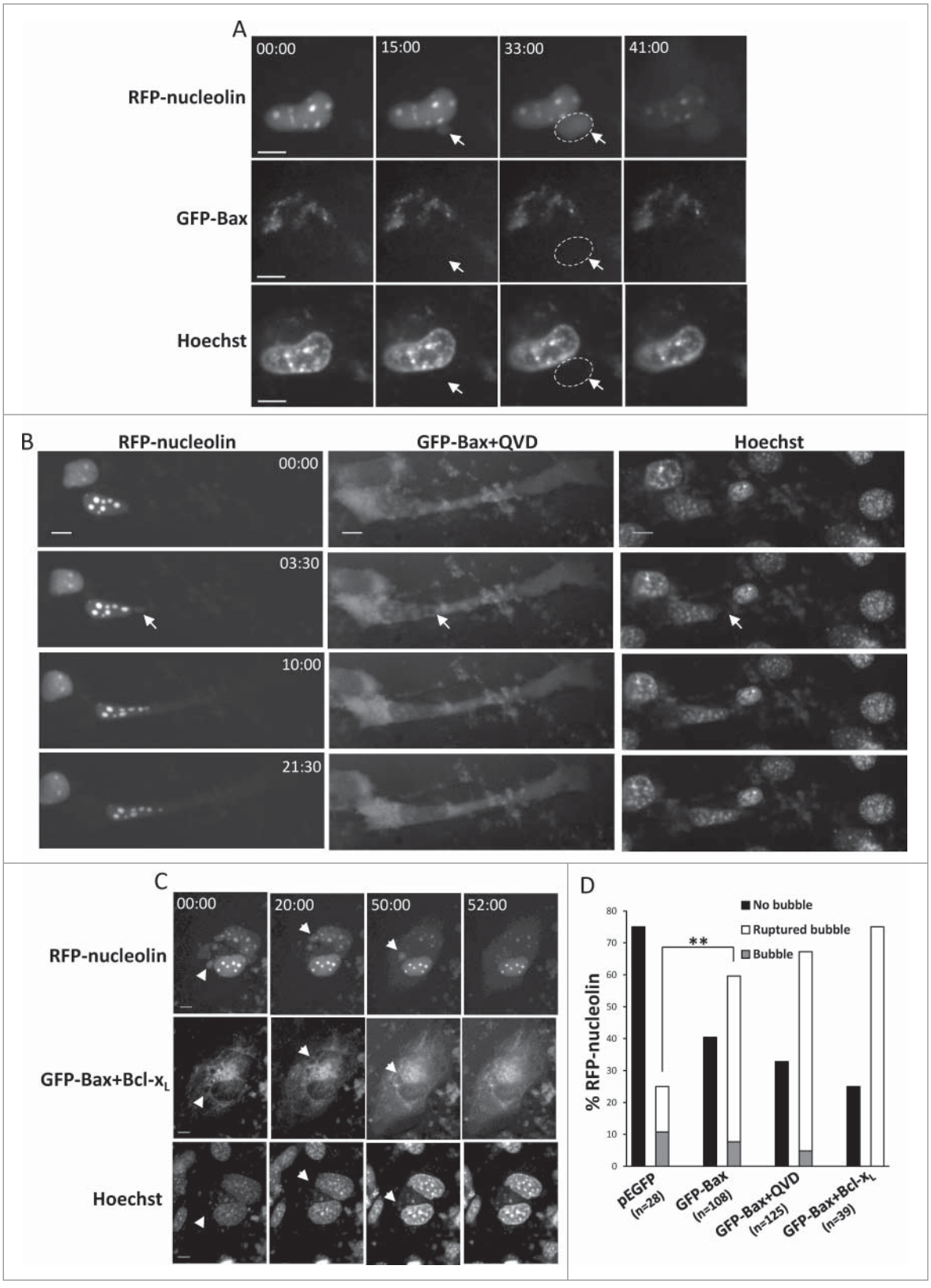

Figure 4. For figure legend see page 533.

pEGFP-expressing cells ($p < 0.0001$, Pearson Chi-square test) (**Fig. 5**). Mutations in the BH3 (L63E and ΔIGDE) and homo-oligomerization (63-65A) domains, or deletion of helices 5 and 6 (Δα5/6) significantly inhibited this redistribution ($p < 0.0001$, Pearson Chi-square test), as previously described.[18] Only the Bax mutant 63-65A inhibited nuclear bubble appearance ($p = 0.02$, Fisher's exact test). The other BH3 mutants or Δα5/6 showed a significant increase in bubble formation ($p < 0.02$, Fisher's exact test), probably due to a delay in bubble rupturing. Taken together, these results suggest that Bax regulates both the generation and rupture of nuclear bubbles. While homo-oligomerization of Bax seems to be required for the bubble formation process, other motives of the BH3 domain and helices α5/6 may trigger bubble rupture.

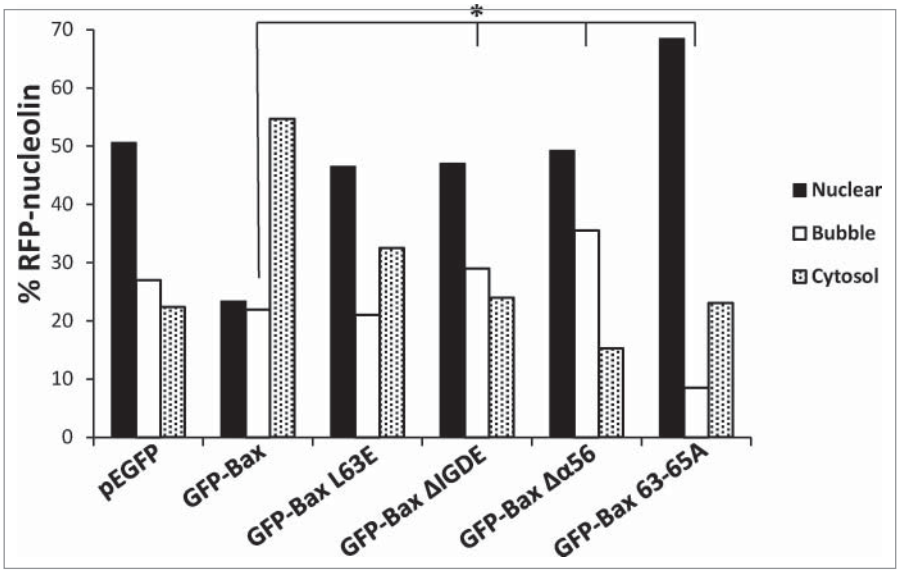

Figure 5. Identification of the Bax domains needed for promoting SIGRUNB. Bax/Bak DKO MEFs were co-transfected with RFP-nucleolin together with pEGFP, GFP-Bax or the indicated GFP-Bax mutants in the presence of 20 μM Q-VD-OPH. The cells were fixed 24 h after transfection and stained with Hoechst 33258 dye (to detect the nuclei), and GFP- and RFP-expressing cells were visualized by fluorescence microscopy. The number of cells exhibiting RFP-nucleolin only in the nuclei (nuclear), bubbles or cytosol was determined microscopically. The results are expressed as percentage of cells exhibiting nuclear, bubble or cytosolic RFP-nucleolin out of total RFP-expressing cells (n = 500 cells; 5 independent experiments). Pearson Chi-square test revealed significant differences ($P < 0.0001$) in the percentages of cells showing nuclear, bubble and cytosolic distribution of RFP-nucleolin between pEGFP and GFP-Bax and between GFP-Bax and each of the Bax mutants. Fisher's exact test of percentage of bubbles revealed significant differences (*$P < 0.05$) between GFP-Bax and GFP-Bax ΔIGDE, GFP-Bax Δα5/6 and GFP-Bax 63-65A.

The question remained how Bax, which is primarily localized to mitochondria, was able to regulate a nuclear process such as SIGRUNB. Since part of Bax had previously been reported to reside on the NE,[24,25] we envisaged the possibility that it might trigger SIGRUNB from that site. We therefore used a Bax variant that was targeted to the outer surface of the ONM of the NE via the KASH domain.[18] Bax/Bak DKO MEFs were co-transfected with RFP-nucleolin and FLAG-Bax KASH or the control vector GFP-mini-nesprin-2G (a KASH-domain-containing protein) vector and SIGRUNB was monitored 24 h after transfection by live cell imaging. As previously reported,[18] FLAG-Bax KASH localized to the NE (marked by NPC proteins) (**Fig. 6A**) but was also detected in surrounding regions. Expression of FLAG-Bax KASH induced significantly more SIGRUNB than the GFP-mini-nesprin-2G control as determined by the percentage of cells exhibiting ruptured or unruptured bubbles during recording ($p = 0.0003$, Fisher's exact test) (**Fig. 6B**). Similarly, a significantly higher percentage of cytosolic RFP-nucleolin (and lower number of nuclear RFP-nucleolin) was detected in fixed FLAG-Bax KASH as compared to GFP-mini-nesprin-2G expressing cells ($p < 0.0001$, Pearson Chi-square test, **Fig. 6C**). We also tested the role of the BH3 domain and helices α5/6 in the SIGRUNB action of FLAG-Bax KASH. As with GFP-Bax, the L63E and Δα5/6 mutations inhibited FLAG-Bax KASH-induced bubble rupture, since less cytosolic RFP-nucleolin and more nuclear bubbles were seen in the mutants as compared to FLAG-Bax KASH cells (**Fig. 6C**) ($p < 0.0001$, Pearson Chi-square test). This indicates that the BH3 and pore-forming domains are also needed for the bubble-rupturing effect of FLAG-Bax KASH. Taken together, these results suggest that targeting Bax to the NE can induce SIGRUNB by a mechanism resembling that of WT Bax.

Figure 4 (See previous page). Restoration of Bax expression in Bax/Bak DKO MEFs promotes SIGRUNB in a caspase- and $Bcl\text{-}x_L$-independent manner. Bax/Bak DKO MEFs were co-transfected with RFP-nucleolin and pEGFP or with RFP-nucleolin and GFP-Bax in the absence (**A**) or presence (**B**) of 20 μM Q-VD-OPH (QVD) or together with $Bcl\text{-}x_L$ (**C**). After 24 h, Hoechst 33342 was added to the culture medium and RFP-nucleolin, GFP-Bax and Hoechst fluorescence-expressing cells were monitored by live-cell time-lapse microscopy at 30-s intervals. Selected (still images from time lapse imaging) from each experiment are shown from the same field visualized separately for detection of RFP-nucleolin, GFP-Bax and Hoechst (**A** and **C** are from **Vid. S4** and **S5**). Note that the bubbles (arrows) do not contain DNA. The dashed oval in (**A**) indicates the position of a DNA-lacking nuclear bubble (no Hoechst staining). Indicated time points (min:s) are expressed relative to the first image selected for presentation (t = 00:00) which corresponds to the image captured 44, 4 or 0 min into the recording (for **A**, **B** and **C**, respectively). Bar = 10 μm. (**D**) Quantification of the percentage of cells exhibiting nuclear bubbles (bubble), nuclear bubbles that ruptured (ruptured bubble) or that did not exhibit bubbles (no bubble) during recording. The number (n) of cells that were monitored for each treatment is indicated. Fisher's exact test of percentage of bubbles (ruptured bubble and bubble) revealed a significant difference (**$p = 0.001$) between GFP-Bax and pEGFP. The results shown are from 2, 3, 2, and 3 independent experiments for pEGFP, GFP-Bax, GFP-Bax+QVD and GFP-Bax+ $Bcl\text{-}x_L$ treatments respectively.

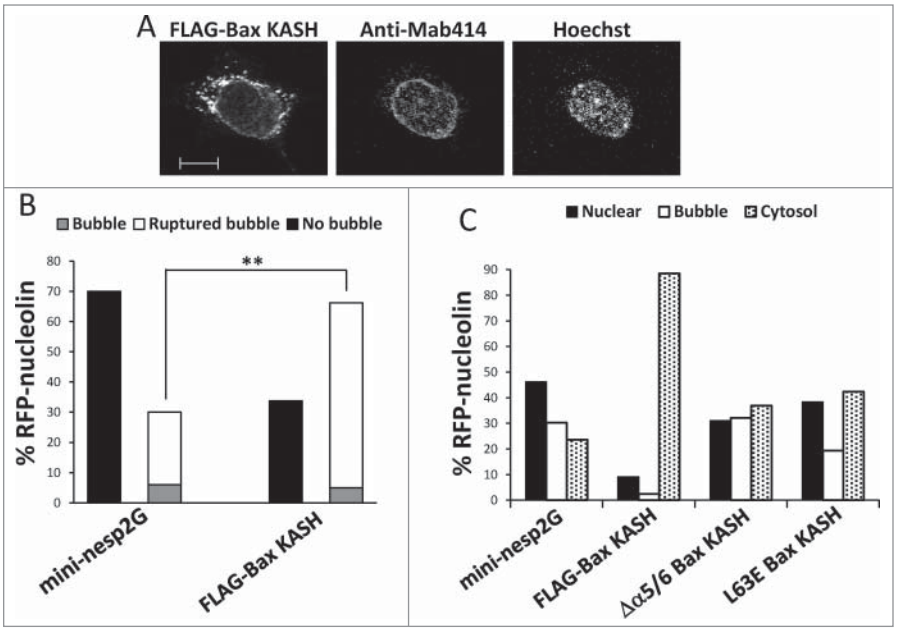

Figure 6. Bax KASH induces generation and rupture of nuclear bubbles, which are inhibited by the L63E and Δα5/6 mutations. (**A**) FLAG-Bax KASH is associated with the NE. Bax/Bak DKO MEFs were transfected with FLAG-Bax KASH and 24 h later were stained with anti-FLAG antibody, Mab414 antibody (to detect NPC) and Hoechst 33258 dye (to detect the nuclei). Thereafter, the cells were visualized by confocal fluorescence microscopy. Presented results are from a representative experiment (out of at least 3 independent experiments). Bar = 10 μm. (**B**) Bax/Bak DKO MEFs were co-transfected with RFP-nucleolin together with GFP-mini-nesprin-2G (mini-nesp2G) or FLAG-Bax KASH. Hoechst 33342 was added to the culture medium 24 h later, and RFP-nucleolin and Hoechst fluorescence was monitored by time-lapse microscopy. The presented results are quantification of the percentage of cells exhibiting bubbles, bubbles that ruptured (ruptured bubble), or no bubbles (no bubble) during the recording period (30-s intervals) out of all recorded RFP-nucleolin-expressing cells. Fisher's exact test of percentage of bubbles (ruptured bubble and bubble) revealed significant differences (**$p = 0.0003$) between GFP-mini-nesprin-2G and FLAG-Bax KASH. (**C**) Bax/Bak DKO MEFs were co-transfected with RFP-nucleolin together with GFP-mini-nesprin-2G (mini-nesp2G), FLAG-Bax KASH or the indicated FLAG-Bax KASH mutants. The cells were fixed and stained with Hoechst 33258 dye and anti-FLAG (to detect Bax KASH-and Bax KASH mutant-expressing cells) 24h later. RFP-nucleolin distribution in the nucleus, bubbles and cytosol in the transfected cells was determined microscopically. The results are expressed as the percentage of RFP-nucleolin in the nuclei, bubbles and cytosol for each treatment out of the respective RFP-nucleolin-expressing cells (n = 500 cells; 5 independent experiments). Pearson Chi-square test revealed significant differences ($p < 0.0001$) in the percentage of nuclear, bubble and cytosolic distribution of RFP-nucleolin between GFP-mini-nesprin-2G and FLAG-Bax KASH, or between FLAG-Bax KASH and each of FLAG-Bax KASH mutants.

Characterization of the Stress-induced Nuclear Bubbles

We further characterized the properties and integrity of the NE in nuclear bubbles. For that purpose, Bax/Bak DKO MEFs were co-transfected with FLAG-Bax and GFP- or RFP-nucleolin. To reduce cell death, the caspase inhibitor Q-VD-OPH (20 μM) was added to the transfected cells. Notably, as mentioned above this treatment does not affect SIGRUNB. The distributions of endogenous lamin A/C, the INM protein emerin and NPC proteins were then examined in fixed cells displaying GFP- nucleolin- but not DNA-containing bubbles. The results show that in Bax non-expressing cells (indicated by the absence of GFP-nucleolin), lamin A/C, emerin and NPC proteins were mainly localized as expected to the nuclear rim. However, in Bax-expressing cells (indicated by expression of GFP-nucleolin) lamin A/C distribution was impaired, as indicated by lamin A/C irregular distribution all over the NE. In addition, lamin A/C was excluded from the site of nuclear bubble protrusion. Some NE regions exhibited accumulation of lamin A/C and punctuated cytosolic lamin A/C staining was observed in many cells (**Fig 7A** and **Fig. S5A**). Expression of Bax also affected emerin and NPC distribution. Emerin levels were substantially reduced in the nucleus and patches of emerin appeared in the cytosol (**Fig 7A** and **Fig. S5B**). NPC were redistributed and appeared also in the nucleoplasm (**Fig 7A**). Notably, all these proteins were absent from the bubble interior and rim. Next we examined whether the nuclear bubbles are surrounded by NE membranes. As markers for the INM of the NE, we used mCherry-LAP2β and GFP-SUN2. However, when overexpressed these 2 fusion proteins may also stain the ONM. We therefore used TAP1(1-6)-GFP (a marker for ER/ONM) as an additional marker for the ONM. Bax/Bak DKO MEFs were co-transfected with FLAG-Bax and each of these NE markers together with RFP-nucleolin or GFP-necleulin. After 24 h, the transfected cells were fixed and analyzed by fluorescence microscopy. The mCherry-LAP2β and GFP-SUN2 did not only localize in the NE and the nucleoplasm but also around the bubbles, in particular at the budding edges (**Fig. 7B**). Similarly, TAP1(1-6)-GFP was detected at the periphery of the bubbles in addition to its expected cytosolic tubular (ER/ONM) distribution (**Fig. 7B**). These results indicate that the FLAG-Bax-induced nuclear bubbles are encapsulated by NE membrane, probably by both the inner and outer membranes and that these membranes, are devoid of NPCs and some other NE proteins.

The Role of Lamin A/C in The SIGRUNB

To further characterize if SIGRUNB could be caused by a disturbance of the lamin A/C network and how this depends on Bax, we examined the ability of lamin A variants associated with human disease to promote SIGRUNB/NPR in Bax/Bak DKO MEFs. The following lamin A variants were used: N195K [found

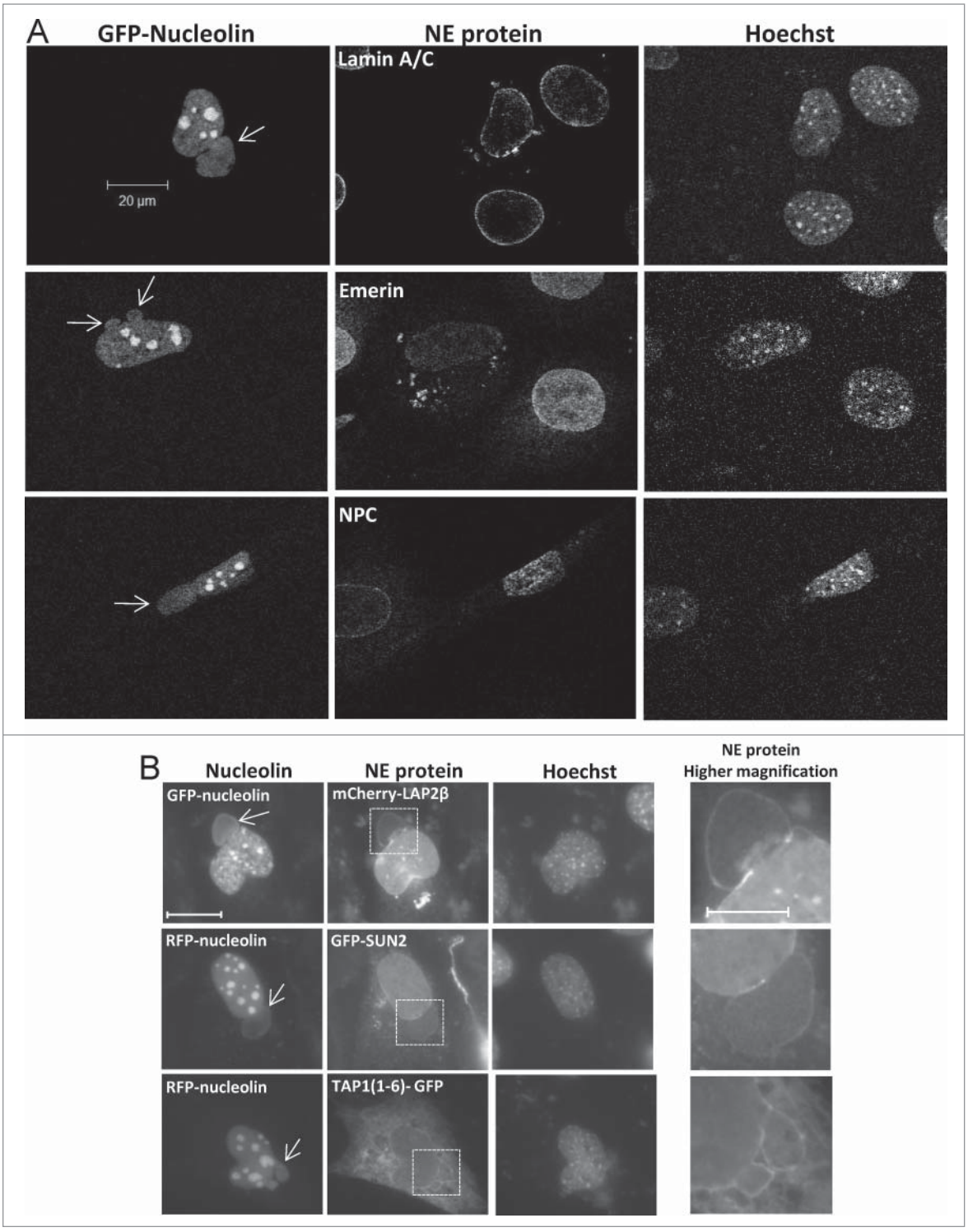

Figure 7. Stress-induced nuclear bubbles are encapsulated by impaired NE. Bax/Bak DKO MEFs were co-transfected with the expression vectors corresponding to FLAG-Bax together with RFP-nucleolin or GFP-nucleolin alone (for assessing endogenous NE proteins) and each of the indicated fluorescence versions of NE-associated proteins (for assessing nuclear bubble encapsulation) in the presence of 20 μM Q-VD-OPH. The cells were fixed and stained with Hoechst 33258 dye (to detect the nuclei) 24 h after transfection. The endogenous proteins were detected by their corresponding antibodies. Mab414 antibody was used to detect NPCs. The images of the endogenous proteins (**A**) were detected by confocal fluorescence microscopy and those of the overexpressed proteins (**B**) by epi-fluorescence microscopy. The images in each row represent the same field visualized separately for detection of RFP/GFP-nucleolin, the indicated NE protein and Hoechst-stained nuclei. Higher magnifications of the dashed boxed areas in the NE protein panel, which contain the bubble-budding sites, are shown in the right panel (**B**). Arrows indicate the position of the bubbles. Presented results are from representative experiments (each, out of at least 3 independent experiments). Bar = 20 μm or 10 μm for the low and high magnifications, respectively.

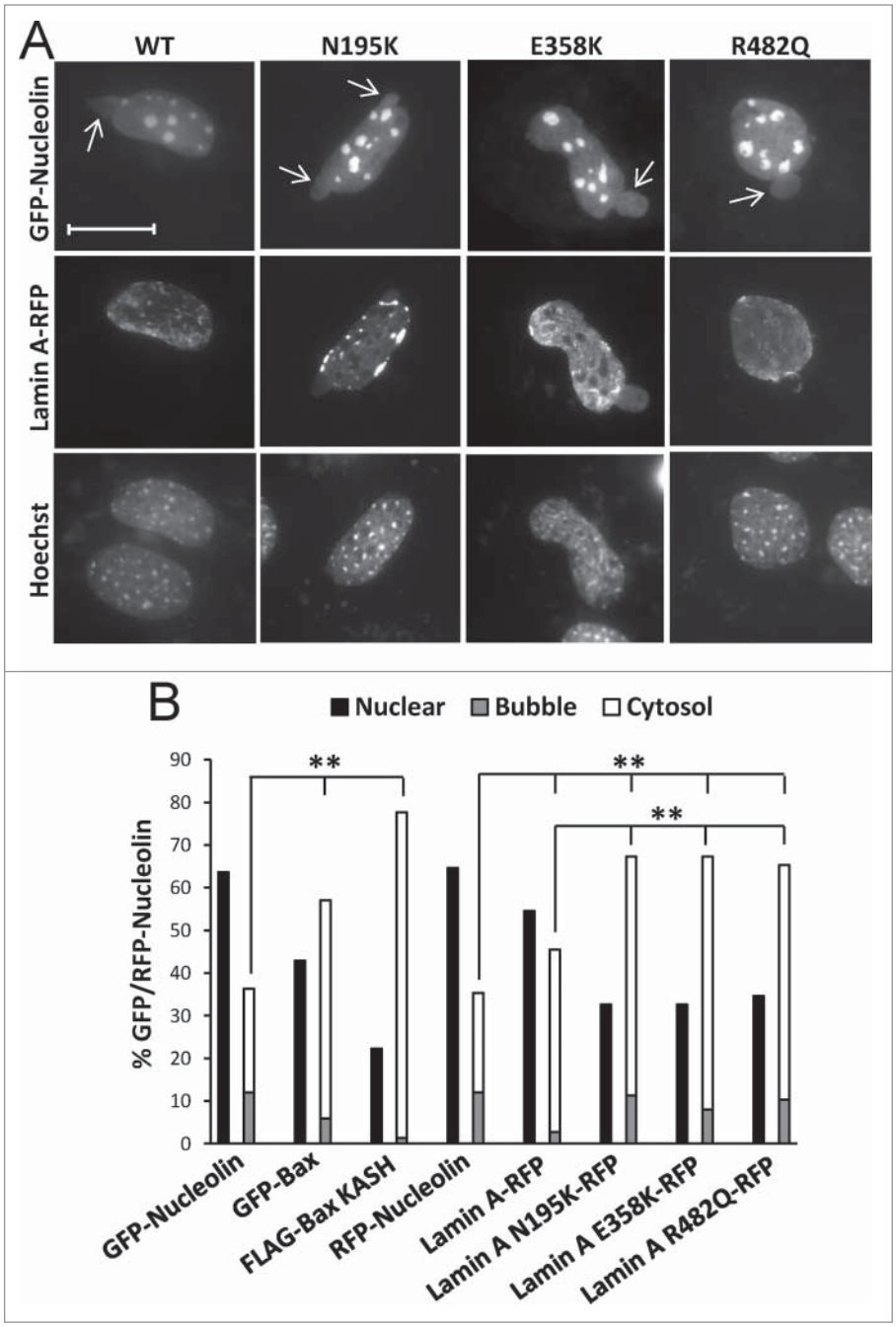

Figure 8. The effect of lamin A variants on SIGRUNB/NPR. Bax/Bak DKO MEFs were co-transfected with lamin A-RFP (WT) or the indicated lamin A mutants together with GFP-nucleolin. The cells were fixed 24 h later, stained with Hoechst 33258 dye and the distribution of lamin A variants in bubble-containing GFP/RFP-expressing cells were visualized by epi-fluorescence microscopy (**A**). Bar = 20 μm. To detect SIGRUNB/NPR (**B**) Bax/Bak DKO MEFs were transfected with RFP-nucleolin or co-transfected with RFP-nucleolin together with GFP-Bax, FLAG-Bax KASH or the indicated lamin A-RFP variants. The cells were fixed 24 h after transfection, stained with Hoechst 33258 dye and RFP-expressing cells were visualized by fluorescence microscopy. GFP/RFP-nucleolin distribution in the nucleus, bubbles and cytosol in the transfected cells was determined microscopically. The results are expressed as the percentage of GFP/RFP-nucleolin in the nuclei, bubbles and cytosol for each transfection out of the respective GFP/RFP-nucleolin-expressing cells (n = 300 cells; 3 independent experiments). Fisher's exact test of percentage of SIGRUNB/NPR (cells exhibiting GFP/RFP-nucleolin in bubbles and cells exhibiting cytosolic GFP/RFP-nucleolin) revealed significant differences (**p = 0.0001) between GFP-nucleolin or RFP-nucleolin to all other treatments; between lamin A-RFP and all the lamin A mutants examined.

in patients with dilated cardiomyopathy/muscular dystrophy], E358K [found in patients with dilated cardiomyopathy/muscular dystrophy] and R482Q [found in patients with familial partial *lipodystrophy*]. In addition, the effect of WT lamin A was examined. Bax/Bak DKO MEFs were transfected with GFP-nucleolin together with each of the above-mentioned lamin A variants fused to RFP. All forms of lamin A showed the expected[26-28] nuclear distribution patterns (**Fig. 8A**). As control experiments, the cells were transfected with GFP-nucleolin plus FLAG-Bax KASH or RFP-nucleolin plus GFP-Bax (or GFP- or RFP-nucleolin alone). SIGRUNB/NPR was examined in fixed cells 24 h post-transfection by assessing the percentage of cells retaining RFP-nucleolin in the nucleus, the percentage of cells exhibiting nuclear bubbles-containing GFP/RFP-nucleolin but not DNA (representative images are shown in **Fig. 8A**), and the percentage of cells containing cytosolic GFP/RFP-nucleolin (an indicative of bubble rupture). As expected, the expression of GFP-Bax and FLAG-BAX KASH significantly ($p < 0.0001$, Fisher's exact test) increased the percentage of cells exhibiting NPR/SIGRUNB (GFP/RFP-nucleolin in cytosol or in bubbles) compared to GFP/RFP-nucleolin expressing cells without transfected Bax (**Fig. 8B**). The lamin A variants also increased NPR/SIGRUNB however the effect of the lamin A mutants was modestly but significantly higher than that of lamin A ($p < 0.0001$, Fisher's exact test) (**Fig. 8B**). These findings suggest that impairment in lamin A/C functionality can induce NPR/SIGRUNB in Bax/Bak DKO MEFs in a similar way as Bax overexpression, supporting the notion that this might be basis for Bax-mediated SIGRUNB. Notably, there were some differences in the distribution pattern between the different lamin variants in the bubbles, indicating that subtle differences in the features of the bubbles induced by the different lamin A/C mutants may exist. Accordingly, the E358K mutant and the N195K mutant (to a lower extent) proteins were presented in the bubble interior. The R482Q mutant protein was not

presented in the bubble interior, but in many cases it partially wrapped the bubble.

A possible mechanism by which apoptotic stress could perturb the function of lamin A/C is via caspase-dependent cleavage.[29] However, our finding that caspase inhibition did not prevent SIGRUNB induced by re-expressing WT Bax in Bax/Bak DKO MEFs did not support such a mechanism. We nevertheless monitored lamin A/C cleavage by immunoblot analysis in cisplatin-treated Bax/Bak DKO MEFs as well as in WT MEFs treated or untreated with 20 μM of the general caspase inhibitor Q-VD-OPH and compared it to SIGRUNB determined by live cell imaging. As expected, lamin A/C were cleaved after 17 and 24 h of cisplatin treatment and this cleavage was completely ablated by co-treatment with Q-VD-OPH as well as in Bax/Bak DKO cells (**Fig. S6**). However, Q-VD-OPH (20 μM) did not inhibit the ability of cisplatin to induce SIGRUNB, which was detected in 68% of the cells (38 cells, n = 2) after 17-24 h of cisplatin treatment, indicating that caspase-mediated cleavage of lamin A/C does not play any role in SIGRUNB.

Discussion

The present study identified a new stress response where nuclear proteins are transferred from the nucleus to the cytosol by a Bax-regulated and NPC-independent manner. This process involves impairments of the NE that result in an expansion of the NE and the formation of bubbles that are filled with nuclear proteins but not DNA. These bubbles then rupture to release the nuclear proteins into the cytosol. Strikingly, this stress-induced NE permeabilization effect is not regulated by caspases but by Bax/Bak via a mechanism requiring the BH3 domain and the α5/6 helices of Bax. Moreover, a Bax variant targeted to the NE via a KASH domain is sufficient to induce SIGRUNB. We and others have previously shown that apoptotic stresses promote NPR [For review see ref[10]] and that this process is regulated by Bax.[17,18] Furthermore, it was suggested that NPR/NE perforation during apoptosis is mediated via export through NPCs or by caspase-dependent disruption of NPC components.[11,30] However, our results show that stress-induced NPR, at the experimental systems employed, is mediated by SIGRUNB and is independent of NPCs.

The Molecular Events at the NE

Our study shows that the stress-induced nuclear bubbles are encapsulated, by NE membrane, probably by both inner and outer membrane, although other encapsulating structures cannot be excluded. The distribution of endogenous lamin A/C and the NE proteins emerin and NPCs were markedly impaired in nuclei of cells undergoing Bax-induced SIGRUNB and moreover they were absent from the periphery of the bubbles indicating that the protein content in the structures that encapsulate the bubble was impaired. Furthermore, together with our previous study showing that Bax enhances lamin A mobility,[18] our findings suggest that the bubbles during SIGRUNB are generated due to perturbation of the nuclear lamina and NE proteins. Indeed, we showed here that disease-associated lamin A variants N195K, E358K and R482Q, induced a NPR effect that is similar to that of GFP-Bax expression in Bax/Bak DKO MEFs. These results are in line with previous studies showing that cells lacking the expression of various lamin genes or harboring mutations in lamins[31-35] or lamin-binding proteins such LBR[36] exhibit similar nuclear-associated bubbles. Moreover, a lamin impairment-associated efflux of nuclear proteins has been reported in cells deficient in lamin A or harboring mutations in lamin A,[35] as well as in cells expressing the HIV Vpr protein,[37] in human cancer cells[38] and in muscle cells during Wnt signaling.[39] Finally, membranes of nuclear bubbles induced by expression of LBR mutants have been shown to be devoid of NPCs and SUN proteins.[36] The cause for impairment of lamin and NE proteins is still unknown. We confirm here that it is not due to caspase-mediated cleavage of lamin A/C because caspase inhibition does not inhibit bubble formation but inhibits lamin A/C cleavage. A possible mechanism may involve changes in lamin A/C phosphorylation since this has been shown to regulate the assembly-disassembly of lamin filaments during mitosis.[40] Further studies are needed to address this issue.

Since NPCs were absent from the nuclear bubbles and GFP-nucleolin was rapidly discharged, the release of nuclear proteins from the bubble cannot be mediated by the leakiness of NPCs. It may be rather due to the rupture of the membranes surrounding the bubble. However, we cannot exclude the possibility that some nuclear rupture may also occur without bubble formation[35] and that some nuclear proteins such as H1.2[30] may translocate from the nucleus to the cytosol during apoptosis via the classical export machinery implying NPCs.

A characteristic feature of SIGRUNB was that the bubbles did not contain DNA. The reason for this is unknown, but it may be due to mechanical constraints that prevent large complex structures, such as chromatin, to move into the bubbles.

The Role of Apoptotic Molecules in SIGRUNB

The finding that SIGRUNB is not induced in cisplatin- or camptothecin-treated Bax/Bak DKO MEFs but is re-established upon Bax re-expression suggests that Bax plays an important role in this process. However, we cannot exclude the possibility that Bak has a similar effect, as previous results showed that re-expression of Bak in Bax/Bak DKO MEFs also restored NPR.[17] Further studies are needed to address this point.

Notably, under certain conditions e.g., transfection, SIGRUNB can also occur in the absence of Bax/Bak, although Bax expression substantially enhanced this process. This is probably because these stimuli converge on the same signaling pathway that is regulated by Bax and is analogous to the ability of some apoptotic stimuli to cause cytochrome *c* release in Bax/Bak DKO MEFs.[18,41] The finding that disease-associated lamin A variants induced NPR in Bax/Bak DKO MEFs supports this notion. The later also imply that lamin A impairment is downstream of Bax action.

The impact of Bax on SIGRUNB was not a consequence of cell death for the following reasons: (1) it was observed in healthy looking cells before any signs of apoptosis, (2) it occurred in cells treated with the caspase inhibitor Q-VD-OPH or in cells co-transfected with Bcl-x_L, which is known to inhibit apoptosis, and (3) it was also seen in cells transfected with FLAG-Bax KASH, which does not induce cell death.[18] The inability of Bcl-x_L to counteract Bax-initiated SIGRUNB, despite its effectiveness in inhibiting cell death [as indicated by the healthy appearance of the GFP-nucleolin/Bax/Bcl-x_L co-transfcted cells], indicates that the SIGRUNB promoting activity of Bax differs from its canonical impact on cell death and MOMP. Nonetheless, the 2 effects might share similar modes of Bax action, because protein domains such as the BH3 domain and helices α5/6, which are known to be necessary for Bax-induced MOMP and cell death, are also needed for NPR[18] and Bax-induced SIGRUNB. Interestingly while the 63-65A mutation [known to inhibit homo-oligomerization[21]] suppressed bubble formation, the Δα5/6 mutation [known to inhibit pore-formation[22]] interfered with bubble rupture. These results indicate that Bax regulates both bubble formation and rupture via its homo-oligomerization and pore-forming activities, respectively.

To determine whether Bax could directly act on the NE to induce SIGRUNB, we targeted Bax to the outer surface of the NE by fusing it to a KASH domain. Similar to WT Bax, FLAG-Bax KASH was able to trigger SIGRUNB. Moreover, the same functional domains, i.e. BH3 and helices α5/6, were required for this activity. The effect of FLAG-Bax KASH on SIGRUNB is unlikely to be caused by impairing LINC complexes in a dominant negative manner since ectopically expressing the KASH domain in the context of another protein, mini-nesprin 2G, was ineffective in promoting SIGRUNB (see **Fig. 6B**). Notably, FLAG-Bax KASH was not exclusively expressed in the NE. Thus the possibility that FLAG-Bax KASH can promote SIGRUNB from non-NE sites, such as the ER cannot be excluded. Nonetheless a NE localization of Bax has been reported in both healthy[42-44] and apoptotic cells.[24,25,45] Thus, we postulate that in response to apoptotic stimuli, Bax not only causes permeabilization of the mitochondrial and ER membranes[46] to release apoptogenic factors, but may also acts, at least in part, on the NE to trigger SIGRUNB. Interestingly, the LINC complex matefin/SUN1 protein in *Caenorhabditis elegans* has been shown to be required to recruit the pro-apoptotic protein CED-4 to the NE.[47] This indicates that the LINC complex might be involved in death signaling emerging from the NE and that in analogy, it may also play a role in the effect of Bax on SIGRUNB. However, we cannot exclude an indirect effect of Bax on the NE either from mitochondria or by disrupting the cytoskeleton and thus perturbing the nuclear lamina via the LINC complex. Further studies are needed to address this issue.

The results presented here show that generation and rupture of nuclear bubbles are part of the cell's response to apoptotic stress. However, despite its association with cell death, SIGRUNB is not sufficient to induce apoptosis. Rather, it may amplify apoptosis by releasing nuclear proteins, such as histone H1.2[30] and NPM[48] into the cytoplasm where they act in cooperation with known apoptosis players of the canonical intrinsic and extrinsic signaling pathways. Whether this is needed for the cells to either cope with stress or enhance an apoptotic response will have to be unraveled in future studies.

Materials and Methods

Materials

All reagents were purchased from Sigma-Aldrich unless otherwise specified. Quinoline-Val-Asp(OMe)-CH_2-OPH (Q-VD-OPH) (catalog number: OPH001)was purchased from R&D Systems Inc.

Cell culture

WT, Bax/Bak DKO MEFs and WT MEFs stably expressing GFP-nucleolin (GN-WT MEFs) [17] were grown in high-glucose Dulbecco's modified Eagle's medium (DMEM) supplemented with 10% heat-inactivated fetal calf serum. Bax/Bak DKO MEFs stably expressing GFP-nucleolin (GN-DKO MEFs) were generated by co-transfection of pEGFP-nucleolin and PGK-Puro expression vectors into Bax/Bak DKO MEFs followed by selection for GFP-nucleolin-expressing and puromycin-resistant clones using 2 mg/ml puromycin.

Plasmids

The expression vectors used in this study were: pEGFP (Clontech Laboratories), pEGFP-Bax (GFP-Bax) and FLAG-Bax (prepared as described previously[49]; FLAG-Bcl-x_L was prepared as described previously[50]; GFP-Bax L63E, GFP-Bax ΔIGDE, GFP-Bax Δα5/6, FLAG-Bax KASH, FLAG-Δα5/6 Bax KASH and FLAG-L63E Bax KASH were prepared as described previously[18]; GFP-Bax 63-65A[51] was a gift from Xu Luo (University of Nebraska Medical Center, Omaha, NE, USA); mCherry-LAP2β was a gift from **Eran Bacharach** (**Tel Aviv University, Tel Aviv, Israel**), **RFP**-lamin A[26], GFP-mini-nesprin-2G[52], GFP-SUN2[52]; GFP-nucleolin[53] and RFP-nucleolin[54] were a gift from Ronit Pinkas-Kramarski (Tel Aviv University), pTAP1(1-6)-GFP[55] was a gift from Jacques Neefjes (Netherlands Cancer Institute, Amsterdam, The Netherlands). The generation of WT prelamin A fused to RFP was described in ref.[26] The generation of the prelamin A N195K, E358K and R482Q mutants fused to RFP was described in ref.[27]

Transfection

The different MEF cell lines were transfected using Lipofectamine (Invitrogen, Life Technologies) (catalog number: 18324-012), according to the manufacturer's instructions. One day before transfection, the cells were seeded at a density of 10^5 cells per well in 12-well plates. When transfected cells were treated with Q-VD-OPH, it was added 5 h after the addition of transfection reagents. The ratios of the different DNA vectors were as follows: 1:1 for GFP-Nucleolin or RFP-Nucleolin/pcDNA3, pEGFP, GFP-Bax, GFP-Bax mutants, FLAG-Bax KASH, FLAG-Bax KASH mutants, GFP-mini-nesprin-2G or Lamin A-mutants; 1:1:1 for RFP-nucleolin/GFP-Bax/FLAG-Bcl-x_L; 1:1:1

for GFP-nucleolin or RFP-nucleolin/FLAG-Bax/GFP-SUN2, mCherry-LAP2β or pTAP1(1-6)-GFP; 1:1 for pEGFP/FLAG-Bax KASH

Live-cell imaging

Cells were plated on a 35-mm glass-bottom dish at 2×10^5 cells per dish (Greiner Bio-One) (catalog number: 627860). After 24 h, the growth medium was replaced with regular growth medium without phenol red and the cells were untreated or treated with 25 μM cisplatin or 1 μM camptothecin, or transfected. When loss of plasma membrane integrity was assessed PI (5 μg/ml) or Hoechst 33258 (1 μg/ml) was added to the culture medium before recording. Healthy-looking cells were monitored 15–24 h later for a period of 1 to 2 h at 30-s intervals using sequential excitation of GFP, RFP and Hoechst, at 471, 561 and 405 nm, respectively. The microscope was in a 37°C temperature-controlled chamber with 5% CO_2 atmosphere. The imaging set-up consisted of an iMIC (TILL Photonics) inverted microscope with an air 20X objective NA = 0.5 (Olympus), a Polychrome V system (TILL Photonics), and an ANDOR iXon DU 888D EMCCD camera (Andor). The equipment was controlled by Live Acquisition Software (TILL Photonics). Images were acquired using Metamorph software (Molecular Devices) and analyzed and annotated using ImageJ software, a Java-based image-processing program developed at the National Institutes of Health (rsbweb.nih.gov/ij).

MitoTracker red staining

Cells were plated on a 35-mm glass-bottom dish at 2×10^5 cells per dish. 28 h later, 100 nM MitoTracker® Red (Life Technologies) (catalog number: M-7512) was added to the culture medium, and 15 min later the growth medium was replaced with regular growth medium without phenol red. After additional 5 h the cells were treated with 25 μM cisplatin.

Immunofluorescence staining

Cells were grown in 12-well plates, 10^5 cells per well, on 18-mm cover slips coated with collagen. After treatments, cells were fixed and stained with the different antibodies and Hoechst dye 33258, as described previously.[56] Next, the cells were incubated with the following primary antibodies: mouse anti-NPM (Invitrogen) (catalog number: 32-5200)), mouse anti-FLAG M5 (Sigma-Aldrich) (catalog number: F 4042), mouse anti-Mab414 (Abcam) (catalog number: ab24609), mouse anti-histone H1 (Santa Cruz Biotechnology) (catalog number: sc-8030), mouse anti-PGC-1α (4C1.3) (Calbiochem) (catalog number: ST1202), mouse anti-lamin A/C (Sigma-Aldrich) (catalog number: SAB4200236) and rabbit anti-emerin (Santa Cruz Biotechnology) (catalog number: sc-15378). Fluorescent images were captured with a fluorescence microscope (Nikon ECLIPSE TE2000-S) connected to a CCD camera (CoolSNAP HQ, RoPER Scientist) with plan Apo VC 60X/1.4 oil-emersion objective using Image-Pro PLUS (version 4.5.1) (Media Cybernetics) software and exported to Photoshop (Adobe). To determine the percentage of cells exhibiting nuclear, bubble or cytosolic RFP-nucleolin, the fluorescently stained cells were counted under a fluorescence microscope. Confocal fluorescent images were obtained using a Meta Zeiss LSM 510 confocal microscope using Zeiss X63 NA 1.4 objective lens. Images were acquired with Zeiss LSM Image Browser version 4.2.0.121.

Immunoblotting

WT and DKO MEFs were untreated or treated with 25 μM cisplatin in the presence or absence of 20 μM QVD-OPH. At different time points, total cell lysates were prepared with homogenization buffer (20 mM phosphate buffer pH 7.4, 5 mM EDTA, 5 mM β-mercaptoethanol) and 50 μg proteins from each treatment was subjected to SDS-PAGE (12.5%) and electroblotted onto supported nitrocellulose. Each blot was blocked for 1 h in 10 mM Tris base, 150 mM NaCl containing 5% fat-free milk, then incubated for 16 h at 4°C with the primary antibody. Mouse anti-lamin A/C (Sigma-Aldrich) or mouse anti-actin (MP Biomedicals) (catalog number: 69100) was used as primary antibody. Gout anti mouse (1:10,000) IgG peroxidase conjugate (Jackson Immunoresearch Laboratories Inc.) were used as second antibody. The blots were developed using chemiluminescence.

Statistical Analysis

Statistical significance was determined based on 2-tailed Fisher's Exact test or Pearson Chi-square test (df = 2). Values of $p < 0.05$ were considered statistically significant.

Disclosure of Potential Conflicts of Interest

No potential conflicts of interest were disclosed.

Acknowledgments

We thank Prof. Andreas Strasser, The Walter and Eliza Hall Institute of Medical Research, Parkville, Victoria, Australia, for providing the Bax/Bak DKO MEFs, Prof. Xu Luo, Eppley Institute for Cancer Research, University of Nebraska Medical Center, Omaha, NE, USA, for providing the GFP-Bax 63-65A plasmid, Prof. Rechavi Gideon, Tel Aviv University, Tel Aviv Israel, for providing the anti-LAP2β antibody, Prof. Eran Bacharach, Tel Aviv University, for providing the mCherry-LAP2β plasmid, Prof. Ronit Pinkas-Kramarski, Tel Aviv University, for providing the GFP-nucleolin and RFP-nucleolin plasmids and Jacques Neefjes, Netherlands Cancer Institute, Amsterdam, The Netherlands, for providing the pTAP1(1-6)-GFP plasmid.

Funding

This work was supported by the Spemann Graduate School of Biology and Medicine (SGBM) (GSC-4) and the Excellence Cluster BIOSS (EXC-294) funded by the DFG (to C. Borner). H.J. Worman was supported by NIH/NIAMS grant AR048997.

Supplemental Material

Supplemental data for this article can be accessed on the publisher's website: http://www.tandfonline.com/kncl

References

1. Walde S, Kehlenbach RH. The Part and the Whole: functions of nucleoporins in nucleocytoplasmic transport. Trends Cell Biol 2010; 20:461-9; PMID:20627572; http://dx.doi.org/10.1016/j.tcb.2010.05.001.
2. Wente SR, Rout MP. The nuclear pore complex and nuclear transport. Cold Spring Harb Perspect Biol 2010; 2:a000562; PMID:20630994; http://dx.doi.org/10.1101/cshperspect.a000562.
3. Prokocimer M, Davidovich M, Nissim-Rafinia M, Wiesel-Motiuk N, Bar DZ, Barkan R, Meshorer E, Gruenbaum Y. Nuclear lamins: key regulators of nuclear structure and activities. J Cell Mol Med 2009; 13:1059-85; PMID:19210577; http://dx.doi.org/10.1111/j.1582-4934.2008.00676.x.
4. Bank EM, Gruenbaum Y. The nuclear lamina and heterochromatin: a complex relationship. Biochem Soc Trans 2011; 39:1705-9; PMID:22103511; http://dx.doi.org/10.1042/BST20110603.
5. Broers JL, Ramaekers FC, Bonne G, Yaou RB, Hutchison CJ. Nuclear lamins: laminopathies and their role in premature ageing. Physiol Rev 2006; 86:967-1008; PMID:16816143; http://dx.doi.org/10.1152/physrev.00047.2005.
6. Wilson KL, Foisner R. Lamin-binding Proteins. Cold Spring Harb Perspect Biol 2010; 2:a000554; PMID:20452940; http://dx.doi.org/10.1101/cshperspect.a000554.
7. Pop C, Salvesen GS. Human caspases: activation, specificity, and regulation. J Biol Chem 2009; 284:21777-81; PMID:19473994; http://dx.doi.org/10.1074/jbc.R800084200.
8. Youle RJ, Strasser A. The BCL-2 protein family: opposing activities that mediate cell death. Nat Rev Mol Cell Biol 2008; 9:47-59; PMID:18097445; http://dx.doi.org/10.1038/nrm2308.
9. Ferrando-May E. Nucleocytoplasmic transport in apoptosis. Cell Death Differ 2005; 12:1263-76; PMID:15861192; http://dx.doi.org/10.1038/sj.cdd.4401626.
10. Lindenboim L, Borner C, Stein R. Nuclear proteins acting on mitochondria. Biochim Biophys Acta 2011; 1813:584-96; PMID:21130123; http://dx.doi.org/10.1016/j.bbamcr.2010.11.016.
11. Ferrando-May E, Cordes V, Biller-Ckovric I, Mirkovic J, Gorlich D, Nicotera P. Caspases mediate nucleoporin cleavage, but not early redistribution of nuclear transport factors and modulation of nuclear permeability in apoptosis. Cell Death Differ 2001; 8:495-505; PMID:11423910; http://dx.doi.org/10.1038/sj.cdd.4400837.
12. Patre M, Tabbert A, Hermann D, Walczak H, Rackwitz HR, Cordes VC, Ferrando-May E. Caspases target only two architectural components within the core structure of the nuclear pore complex. J Biol Chem 2006; 281:1296-304; PMID:16286466; http://dx.doi.org/10.1074/jbc.M511717200.
13. Faleiro L, Lazebnik Y. Caspases disrupt the nuclear-cytoplasmic barrier. J Cell Biol 2000; 151:951-9; PMID:11085998; http://dx.doi.org/10.1083/jcb.151.5.951.
14. Kihlmark M, Imreh G, Hallberg E. Sequential degradation of proteins from the nuclear envelope during apoptosis. J Cell Sci 2001; 114:3643-53; PMID:11707516.
15. Buendia B, Santa-Maria A, Courvalin JC. Caspase-dependent proteolysis of integral and peripheral proteins of nuclear membranes and nuclear pore complex proteins during apoptosis. J Cell Sci 1999; 112 1743-53; PMID:10318766.
16. Bano D, Dinsdale D, Cabrera-Socorro A, Maida S, Lambacher N, McColl B, Ferrando-May E, Hengartner MO, Nicotera P. Alteration of the nuclear pore complex in Ca(2+)-mediated cell death. Cell Death Differ 2010; 17:119-33; PMID:19713973; http://dx.doi.org/10.1038/cdd.2009.112.
17. Lindenboim L, Blacher E, Borner C, Stein R. Regulation of stress-induced nuclear protein redistribution: a new function of Bax and Bak uncoupled from Bcl-x(L). Cell Death Differ 2010; 17:346-59; PMID:19816507; http://dx.doi.org/10.1038/cdd.2009.145.
18. Lindenboim L, Ferrando-May E, Borner C, Stein R. Non-canonical function of Bax in stress-induced nuclear protein redistribution. Cell Mol Life Sci 2013; 70:3013-27; PMID:23475110; http://dx.doi.org/10.1007/s00018-013-1306-4.
19. Zhou H, Hou Q, Chai Y, Hsu YT. Distinct domains of Bcl-XL are involved in Bax and Bad antagonism and in apoptosis inhibition. Exp Cell Res 2005; 309:316-28; PMID:16061221; http://dx.doi.org/10.1016/j.yexcr.2005.06.014.
20. Borner C. The Bcl-2 protein family: sensors and checkpoints for life-or-death decisions. Mol Immunol 2003; 39:615-47; PMID:12493639; http://dx.doi.org/10.1016/S0161-5890(02)00252-3.
21. George NM, Evans JJD, Luo X. A three-helix homo-oligomerization domain containing BH3 and BH1 is responsible for the apoptotic activity of Bax. Gene Dev 2007; 21:1937-48; PMID:17671092; http://dx.doi.org/10.1101/gad.1553607.
22. Heimlich G, McKinnon AD, Bernardo K, Brdiczka D, Reed JC, Kain R, Kronke M, Jurgensmeier JM. Bax-induced cytochrome c release from mitochondria depends on α-helices-5 and -6. Biochem J 2004; 378:247-55; PMID:14614769; http://dx.doi.org/10.1042/BJ20031152.
23. Minn AJ, Kettlun CS, Liang H, Kelekar A, Vander Heiden MG, Chang BS, Fesik SW, Fill M, Thompson CB. Bcl-xL regulates apoptosis by heterodimerization-dependent and -independent mechanisms. EMBO J 1999; 18:632-43; PMID:9927423; http://dx.doi.org/10.1093/emboj/18.3.632.
24. Gajkowska B, Motyl T, Olszewska-Badarczuk H, Godlewski MM. Expression of BAX in cell nucleus after experimentally induced apoptosis revealed by immunogold and embedment-free electron microscopy. Cell Biol Int 2001; 25:725-33; PMID:11482896; http://dx.doi.org/10.1006/cbir.2001.0768.
25. Gajkowska B, Wojewodzka U, Gajda J. Translocation of Bax and Bid to mitochondria, endoplasmic reticulum and nuclear envelope: possible control points in apoptosis. J Mol Histol 2004; 35:11-9; PMID:15323345; http://dx.doi.org/10.1023/B:HIJO.0000020900.86650.89.
26. Ostlund C, Sullivan T, Stewart CL, Worman HJ. Dependence of diffusional mobility of integral inner nuclear membrane proteins on A-type lamins. Biochemistry 2006; 45:1374-82; PMID:16445279; http://dx.doi.org/10.1021/bi052156n.
27. Folker ES, Ostlund C, Luxton GW, Worman HJ, Gundersen GG. Lamin A variants that cause striated muscle disease are defective in anchoring transmembrane actin-associated nuclear lines for nuclear movement. Proc Natl Acad Sci USA 2011; 108:131-6; PMID:21173262; http://dx.doi.org/10.1073/pnas.1000824108.
28. Östlund C, Bonne G, Schwartz K, Worman HJ. Properties of lamin A mutants found in Emery-Dreifuss muscular dystrophy, cardiomyopathy and Dunnigan-type partial lipodystrophy. J Cell Sci 2001; 114:4435-45.
29. Ruchaud S, Korfali N, Villa P, Kottke TJ, Dingwall C, Kaufmann SH, Earnshaw WC. Caspase-6 gene disruption reveals a requirement for lamin A cleavage in apoptotic chromatin condensation. EMBO J 2002; 21:1967-77; PMID:11953316; http://dx.doi.org/10.1093/emboj/21.8.1967.
30. Konishi A, Shimizu S, Hirota J, Takao T, Fan Y, Matsuoka Y, Zhang L, Yoneda Y, Fujii Y, Skoultchi AI, et al. Involvement of histone H1.2 in apoptosis induced by DNA double-strand breaks. Cell 2003; 114:673-88; PMID:14505568; http://dx.doi.org/10.1016/S0092-8674(03)00719-0.
31. Lenz-Bohme B, Wismar J, Fuchs S, Reifegerste R, Buchner E, Betz H, Schmitt B. Insertional mutation of the Drosophila nuclear lamin Dm0 gene results in defective nuclear envelopes, clustering of nuclear pore complexes, and accumulation of annulate lamellae. J Cell Biol 1997; 137:1001-16; PMID:9166402; http://dx.doi.org/10.1083/jcb.137.5.1001.
32. Liu J, Rolef Ben-Shahar T, Riemer D, Treinin M, Spann P, Weber K, Fire A, Gruenbaum Y. Essential roles for Caenorhabditis elegans lamin gene in nuclear organization, cell cycle progression, and spatial organization of nuclear pore complexes. Mol Biol Cell 2000; 11:3937-47; PMID:11071918; http://dx.doi.org/10.1091/mbc.11.11.3937.
33. Sullivan T, Escalante-Alcalde D, Bhatt H, Anver M, Bhat N, Nagashima K, Stewart CL, Burke B. Loss of A-type lamin expression compromises nuclear envelope integrity leading to muscular dystrophy. J Cell Biol 1999; 147:913-20; PMID:10579712; http://dx.doi.org/10.1083/jcb.147.5.913.
34. Vergnes L, Peterfy M, Bergo MO, Young SG, Reue K. Lamin B1 is required for mouse development and nuclear integrity. Proc Natl Acad Sci USA 2004; 101:10428-33; PMID:15232008; http://dx.doi.org/10.1073/pnas.0401424101.
35. De Vos WH, Houben F, Kamps M, Malhas A, Verheyen F, Cox J, Manders EM, Verstraeten VL, van Steensel MA, Marcelis CL, et al. Repetitive disruptions of the nuclear envelope invoke temporary loss of cellular compartmentalization in laminopathies. Hum Mol Genet 2011; 20:4175-86; PMID:21831885; http://dx.doi.org/10.1093/hmg/ddr344.
36. Zwerger M, Kolb T, Richter K, Karakesisoglou I, Herrmann H. Induction of a massive endoplasmic reticulum and perinuclear space expansion by expression of lamin B receptor mutants and the related sterol reductases TM7SF2 and DHCR7. Mol Biol Cell 2010; 21:354-68; PMID:19940018; http://dx.doi.org/10.1091/mbc.E09-08-0739.
37. de Noronha CM, Sherman MP, Lin HW, Cavrois MV, Moir RD, Goldman RD, Greene WC. Dynamic disruptions in nuclear envelope architecture and integrity induced by HIV-1 Vpr. Science 2001; 294:1105-8; PMID:11691994; http://dx.doi.org/10.1126/science.1063957.
38. Vargas JD, Hatch EM, Anderson DJ, Hetzer MW. Transient nuclear envelope rupturing during interphase in human cancer cells. Nucleus 2012; 3:88-100; PMID:22567193; http://dx.doi.org/10.4161/nucl.18954.
39. Speese SD, Ashley J, Jokhi V, Nunnari J, Barria R, Li Y, Ataman B, Koon A, Chang YT, Li Q, et al. Nuclear envelope budding enables large ribonucleoprotein particle export during synaptic Wnt signaling. Cell 2012; 149:832-46; PMID:22579286; http://dx.doi.org/10.1016/j.cell.2012.03.032.
40. Heald R, McKeon F. Mutations of phosphorylation sites in lamin A that prevent nuclear lamina disassembly in mitosis. Cell 1990; 61:579-89; PMID:2344612; http://dx.doi.org/10.1016/0092-8674(90)90470-Y.
41. Wan KF, Chan SL, Sukumaran SK, Lee MC, Yu VC. Chelerythrine induces apoptosis through a Bax/Bak-independent mitochondrial mechanism. J Biol Chem 2008; 283:8423-33; PMID:18230621; http://dx.doi.org/10.1074/jbc.M707687200.
42. Hoetelmans R, van Slooten HJ, Keijzer R, Erkeland S, van de Velde CJ, Dierendonck JH. Bcl-2 and Bax proteins are present in interphase nuclei of mammalian cells. Cell Death Differ 2000; 7:384-92; PMID:10773823; http://dx.doi.org/10.1038/sj.cdd.4400664.
43. Hoetelmans RW. Nuclear partners of Bcl-2: Bax and PML. DNA Cell Biol 2004; 23:351-4; PMID:15231068; http://dx.doi.org/10.1089/104454904323145236.
44. Gajkowska B, Motyl T, Olszewska-Badarczuk H, Gniadecki R, Koronkiewicz M. Structural association of Bax with nuclear matrix and cytomatrix revealed by embedment-free immunogold electron microscopy. Cell Biol Int 2000; 24:649-56; PMID:10964454; http://dx.doi.org/10.1006/cbir.2000.0530.
45. Mandal M, Adam L, Mendelsohn J, Kumar R. Nuclear targeting of Bax during apoptosis in human colorectal cancer cells. Oncogene 1998; 17:999-1007; PMID:9747879; http://dx.doi.org/10.1038/sj.onc.1202020.
46. Wang X, Olberding KE, White C, Li C. Bcl-2 proteins regulate ER membrane permeability to luminal

proteins during ER stress-induced apoptosis. Cell Death Differ 2011; 18:38-47; PMID:20539308; http://dx.doi.org/10.1038/cdd.2010.68.
47. Tzur YB, Margalit A, Melamed-Book N, Gruenbaum Y. Matefin/SUN-1 is a nuclear envelope receptor for CED-4 during Caenorhabditis elegans apoptosis. Proc Natl Acad Sci USA 2006; 103:13397-402.
48. Kerr LE, Birse-Archbold JL, Short DM, McGregor AL, Heron I, Macdonald DC, Thompson J, Carlson GJ, Kelly JS, McCulloch J, et al. Nucleophosmin is a novel Bax chaperone that regulates apoptotic cell death. Oncogene 2007; 26:2554-62; PMID:17072349; http://dx.doi.org/10.1038/sj.onc.1210044.
49. Schinzel A, Kaufmann T, Schuler M, Martinalbo J, Grubb D, Borner C. Conformational control of Bax localization and apoptotic activity by Pro168. J Cell Biol 2004; 164:1021-32; PMID:15037603; http://dx.doi.org/10.1083/jcb.200309013.
50. Kaufmann T, Schlipf S, Sanz J, Neubert K, Stein R, Borner C. Characterization of the signal that directs Bcl-x (L), but not Bcl-2, to the mitochondrial outer membrane. J Cell Biol 2003; 160:53-64; PMID:12515824; http://dx.doi.org/10.1083/jcb.200210084.
51. George NM, Targy N, Evans JJ, Zhang L, Luo X. Bax contains two functional mitochondrial targeting sequences and translocates to mitochondria in a conformational change- and homo-oligomerization-driven process. J Biol Chem 2010; 285:1384-92; PMID:19880508; http://dx.doi.org/10.1074/jbc.M109.049924.
52. Ostlund C, Folker ES, Choi JC, Gomes ER, Gundersen GG, Worman HJ. Dynamics and molecular interactions of linker of nucleoskeleton and cytoskeleton (LINC) complex proteins. J Cell Sci 2009; 122:4099-108; PMID:19843581; http://dx.doi.org/10.1242/jcs.057075.
53. Di Segni A, Farin K, Pinkas-Kramarski R. Identification of nucleolin as new ErbB receptors- interacting protein. PloS One 2008; 3:e2310; PMID:18523588; http://dx.doi.org/10.1371/journal.pone.0002310.
54. Farin K, Di Segni A, Mor A, Pinkas-Kramarski R. Structure-function analysis of nucleolin and ErbB receptors interactions. PloS One 2009; 4:e6128; PMID:19578540; http://dx.doi.org/10.1371/journal.pone.0006128.
55. Vos JC, Reits EA, Wojcik-Jacobs E, Neefjes J. Head-head/tail-tail relative orientation of the pore-forming domains of the heterodimeric ABC transporter TAP. Curr Biol 2000; 10:1-7; PMID:10660295; http://dx.doi.org/10.1016/S0960-9822(99)00257-2.
56. Lindenboim L, Kringel S, Braun T, Borner C, Stein R. Bak but not Bax is essential for Bcl-xS-induced apoptosis. Cell Death Differ 2005; 12:713-23; PMID:15861188; http://dx.doi.org/10.1038/sj.cdd.4401638.